The fast muscle Myosin light chain *mylpfa* is essential for fast muscle function and integrity

Undergraduate Research Thesis

Presented in Partial Fulfillment of the Requirements for graduation “with Honors Research Distinction in Molecular Genetics” in the undergraduate colleges of The Ohio State University

by

Emily Teets

The Ohio State University

April 2018

Project Advisor: Dr. Sharon Amacher, Department of Molecular Genetics

Abstract

The structure and function of muscles are vital to human health and mobility. Muscle fibers contain contractile proteins organized into units called sarcomeres that are necessary for muscle function. Mutations in proteins of the sarcomere, such as in the Myosin regulatory light chains, can lead to degenerative diseases in humans, such as nemaline and cardiac myopathies. These Myosin regulatory light chain proteins regulate Myosin heavy chain protein to alter the kinetics of muscle contraction. I hypothesize that *mylpfa* is necessary not only for Myosin heavy chain regulation, but also vital for sarcomere formation in fast muscle. To test this, we generated knockouts in four zebrafish Myosin light chain genes, *mylpfa*, *mylpfb, myl1a,* and *myl1b*. The *mylpfa*$^{-/-}$ mutants have severe defects in all fast muscle fibers, while sarcomeres in slow muscle fibers appear unaffected. Mutants for the second *Mylpf* in zebrafish, *mylpfb*$^{-/-}$, appear normal, indicating that *mylpfa* is the more important of the two *Mylpf* homologs. Consistent with my hypothesis, *mylpfa*$^{-/-}$ mutant embryos have weakened muscles caused by severely disrupted sarcomere structure. Later, during larval stages, the weakened *mylpfa*$^{-/-}$ mutant muscle fibers degenerate, resulting in loss of fast muscle fibers. Thus, our findings reveal that in addition to their role in muscle contraction, *Mylpf* genes are vital to sarcomere formation and muscle fiber integrity in fast muscles. Further investigation into how *mylpfa* functions in sarcomere assembly and how sarcomere assembly influences fiber integrity may help explain degenerative muscle diseases caused by mutations in sarcomeric proteins.

Introduction

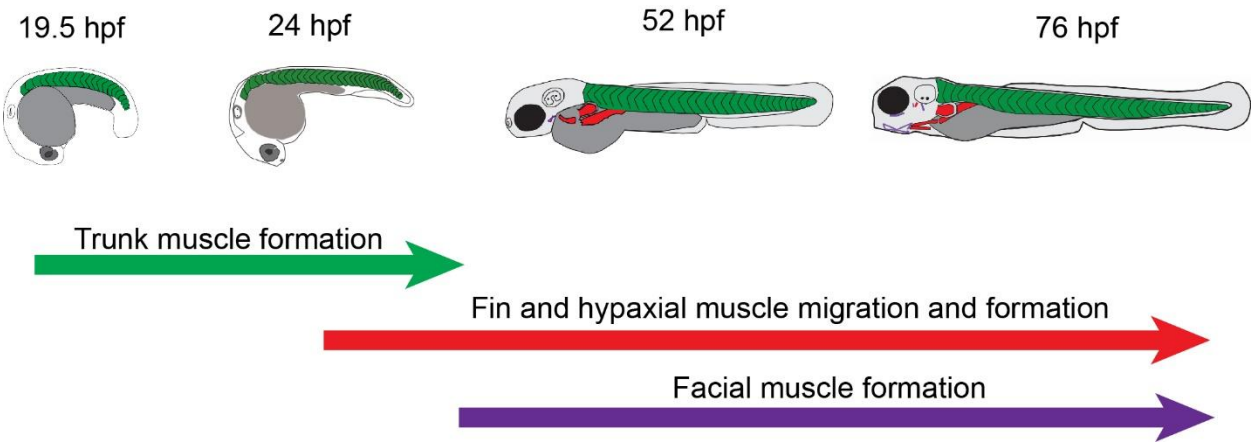

Figure 1. Rapid muscle development in zebrafish

Illustrations of timeline of muscle development in zebrafish from 19.5 hours post fertilization (hpf) and 76 hpf. Green muscle represents trunk muscle, a population of both fast and slow muscle, Red indicates fin and hypaxial muscles, populations of pure fast muscle. Purple are facial muscles and are a mix of fast and slow muscle.

Muscle fibers are long, multinucleated fibers that, span the length of myotomes in skeletal muscle. In zebrafish, trunk muscle forms very rapidly, allowing fish to move within 24 hours post fertilization (hpf). After this initial rapid myogenesis, trunk muscle grows more slowly, and other muscle populations form by 52 to 76 hours post fertilization (hpf) (**Figure 1**) (Haines et al., 2004; Schilling and Kimmel, 1997). Long rod-like structures, known as myofibrils, compose muscle cells. Myofibrils contain the basic structural and contractile units, known as sarcomeres, throughout their length (**Figure 2A**) (Clark et al., 2002; Sanger et al., 2010). Thick filaments of Myosin proteins and thin filaments of Actin make up the sarcomere. The thick filaments ratchet along the thin filaments, pulling them in to shorten the sarcomere. When the sarcomeres throughout the myofibrils shorten, the myofibrils contract, thus contracting the muscles (**Figure 2B**) (Huxley, 2000). I hypothesize that the Myosin light chain *mylpfa*, a component of the thick filaments, is essential for sarcomere assembly, and thereby essential for normal muscle contraction and integrity.

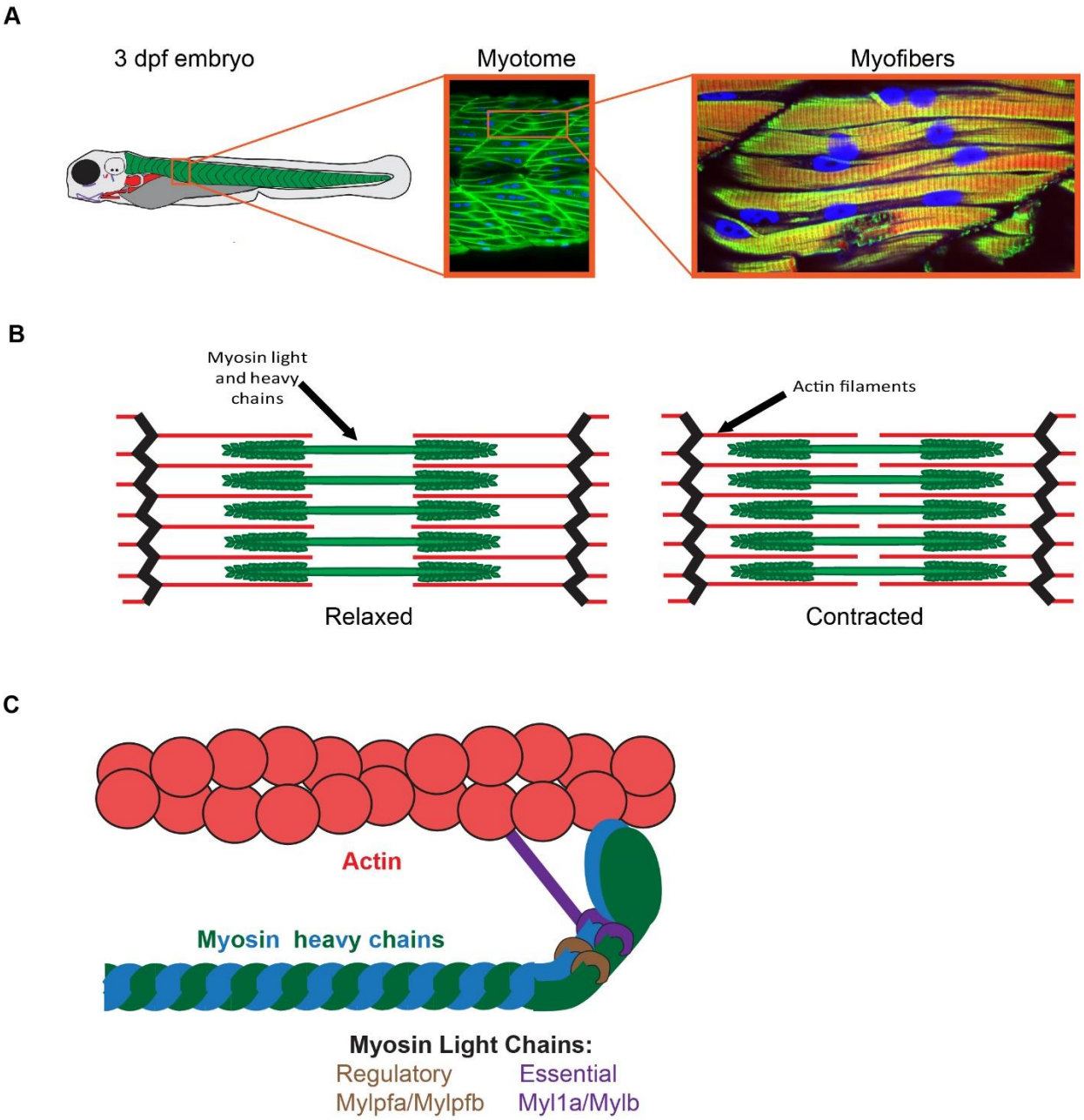

Figure 2. Sarcomeres are the basic contractile unit of muscles.

(A) Illustration of a 3 days post fertilization (dpf) zebrafish embryo. First inset zooms in on the myotome of the trunk muscles. Confocal image shows fast muscles of the trunk (green) and myonuclei (blue). Second inset shows a confocal image of myofibers with Actin (red), Myosin heavy chains (green), and myonuclei (blue) labeled by antibodies. **(B)** Illustration of sarcomere organization. Red thin filaments composed of Actin associate with green thick filaments of Myosins to make up the sarcomeres. **(C)** Illustration of Actin and Myosin interaction. The blue/green head regions of the Myosin heavy chains bind to the Actin (red) and ratchet them to shorten the sarcomere. Two classes of Myosin light chains, the Regulatory light chains (tan) and Essential light chains (purple), bind around the neck of the Myosin heavy chains and regulate the step size of Actin ratcheting.

Several studies spanning many years and using a variety of model organisms, come to propose a three-step model for sarcomere development. In the first step of myofibrillogenesis, pre-myofibrils form along the length of myofibers by the interaction of Actin filaments and non-muscle myosin. Next, muscle Myosin replaces the non-muscle Myosin and another sarcomeric protein, Titin, integrate themselves, forming nascent myofibrils. Third, other sarcomeric proteins that facilitate contraction and cross-link sarcomeric structures layer in, forming mature myofibrils (Du et al., 2003; Sanger et al., 2017). Recent work in *Drosophila* expanded on this model and highlights the importance of tension in the assembly of the sarcomeres. The authors of this study propose that Actin begins to align itself throughout the cell, but that it is not until cell elongation and the tension provided from muscle-tendon junctions that the Actin stretches out to span the length of the cell and associate with thick filaments (Lemke and Schnorrer, 2017). Before sarcomeres span the whole myofibers, micro-contractions may locally generate tension. These micro-contractions of sarcomeric structure throughout the length of the myofibril align the sarcomeres (Weitkunat et al., 2017). I hypothesize that the micro-contractions that align the sarcomeres require Myosin light chains, which are known to be involved in regulating muscle contraction (Takashima, 2009). Thus, in the absence of Myosin light chains, the myofibrils will lack sarcomeric organization and muscle integrity.

I chose to focus on the Myosin light chains due to their known role in sarcomere contraction (Duggal et al., 2015). Myosin heavy chains require the Myosin light chains for normal movement along Actin filaments. Actin enzymatic activity is reduced by 50% and Actin velocity is reduced ten-fold when Myosin heavy chains are stripped of their light chains in vitro (Lowey et al., 1993a). Thus, null mutations in the Myosin light chain genes would be predicted to lead to a lack of the sarcomere contraction that reportedly organizes myofibril structure (Weitkunat et al., 2017). My research focuses on the fast skeletal muscles, which is a muscle type that contracts and fatigues quickly (Schiaffino and Reggiani, 2011; Talbot and Maves,

2016). There are two categories of Myosin light chains within fast muscle: the regulatory light chain (RLC) and the essential light chain (ELC). Both types of light chains bind to the neck region of the skeletal muscle Myosin heavy chain; ELCs bind closest to the force-generating head region, while RLCs bind slightly further away from the head (**Figure 2C**). In humans, the fast muscle RLC is known as *Mylpf* and the ELC is *Myl1.* Myosin light chains in *Drosophila* tune heavy chain activity by changing the ratcheting step size and thereby governing how quickly and forcefully the muscle contracts (Burghardt et al., 2016). In particular, the long isoform of the ELC has an arm that binds to the actin filaments and regulate the ratcheting step size (Wang et al., 2016). Based on the *Drosophila* work, one would expect similar phenotypes of muscle weakness in other species such as mice. Surprisingly, *Myl1* enhancer knockout mice have severe mesodermal defects (Jiang et al., 2002) and mouse *Mylpf*$^{-/-}$ mutants lack muscle at birth (Wang et al., 2007). The severe phenotype of these mice is surprising since Myl1 and Mylpf were predicted to function in sarcomere contraction and not in muscle formation itself. Thus, the role of Myosin light chain gene function remains unclear during vertebrate development. I hypothesize that Myosin heavy chain association with Actin require Myosin light chains and that the force generated by Myosin ratcheting Actin is necessary for proper alignment of sarcomeric structures. Therefore, I predict that upon mutation of Myosin light chains, sarcomeric structure will not form, leading to muscle weakness, loss of muscle integrity, and ultimately to muscle fiber degeneration.

To test this hypothesis, I focused on the Myosin light chain genes expressed in zebrafish fast muscles: *mylpfa, mylpfb, myl1a,* and *myl1b*. Zebrafish are effective model organisms to study the developmental role of Myosin light chains for several reasons: zebrafish have large clutch size, transparent embryos, rapid muscle growth, and have a fiber organization that lets us easily spot the fast muscle fibers. In humans, mixtures of fast and slow muscle fibers make up the muscles. In contrast, zebrafish trunks have spatially separated fast and slow fibers by one

day post fertilization (dpf). Zebrafish have two copies of each fast-expressed Myosin light chain gene. The RLCs in zebrafish fast muscle are *mylpfa* and *mylpfb* and the ELCs are *myl1a* and *myl1b.* Null mutations for all four zebrafish Myosin light chain genes allow us to examine gene function early in the zebrafish development. Using live imaging of these mutant lines, I observed the muscle phenotype in the absence of each of the Myosin light chains.

Together with other members of the Amacher lab, I isolated mutant lines for four of the Myosin light chains expressed in zebrafish fast muscles using CRISPR/Cas9 mutagenesis. Surprisingly, three of the myosin light chain mutants had no phenotype or only mild swimming defects but otherwise appeared like their wild-type siblings. In contrast, I found that *mylpfa*$^{-/-}$ mutants have significantly slower and weakened swimming. In *mylpfa*$^{-/-}$ mutants, Myosin heavy chains mostly fail to associate with Actin, instead forming globs of protein. Thus, my data suggest that *mylpfa* is the critical Myosin light chain for proper Myosin heavy chains and formation of sarcomeres throughout the myofibrils. Eventually, *mylpfa*$^{-/-}$ mutant muscle fibers degenerate, suggesting that without sarcomeric structure, muscle cells lack the integrity needed to maintain long, multinucleated fibers. *mylpfa* is thus necessary for sarcomere formation, and that without *mylpfa,* muscles are weaker and degenerate, perhaps through a mechanism of localized tension throughout the myofibril.

Results

Fast muscle express Myosin light chain genes in similar patterns

Gene homology and images on ZFin indicated that *myl1a*, *myl1b, mylpfa,* and *mylpfb* are expressed in fast muscles (Thisse et al., 2001; Thisse et al., 2004, Rauch et al., 2003). To ensure that these genes truly are fast muscle specific, I examined the mRNA expression patterns of the four fast muscle specific Myosin light chains using *in situ* hybridization. Fluorescent double in situs of each of the four Myosin light chains colabeled with a slow muscle marker show that each of the four Myosin genes have fast muscle-specific expression at 24 hpf (**Figure 3A**). Single chromogenic in situ hybridization shows that the four Myosin light chains are expressed in the fast skeletal muscles of zebrafish as early as 19.5 hpf (**Figure 3B**). The early trunk muscle expression of the four fast muscle-specific Myosin light chain genes differs from the expression of a slow muscle marker in the trunk by the absence of expression down the middle of the trunk alongside the notochord. Expression of all four of the fast Myosin light chain genes is maintained even after fast muscle has matured (52.5 hpf). The migratory muscles of the fin, face, and hypaxial muscles express the four Myosin light chains which form and migrate between the observed timepoints. Therefore, skeletal muscle expresses the four fast muscle-specific Myosin light chains in similar locations and at similar times.

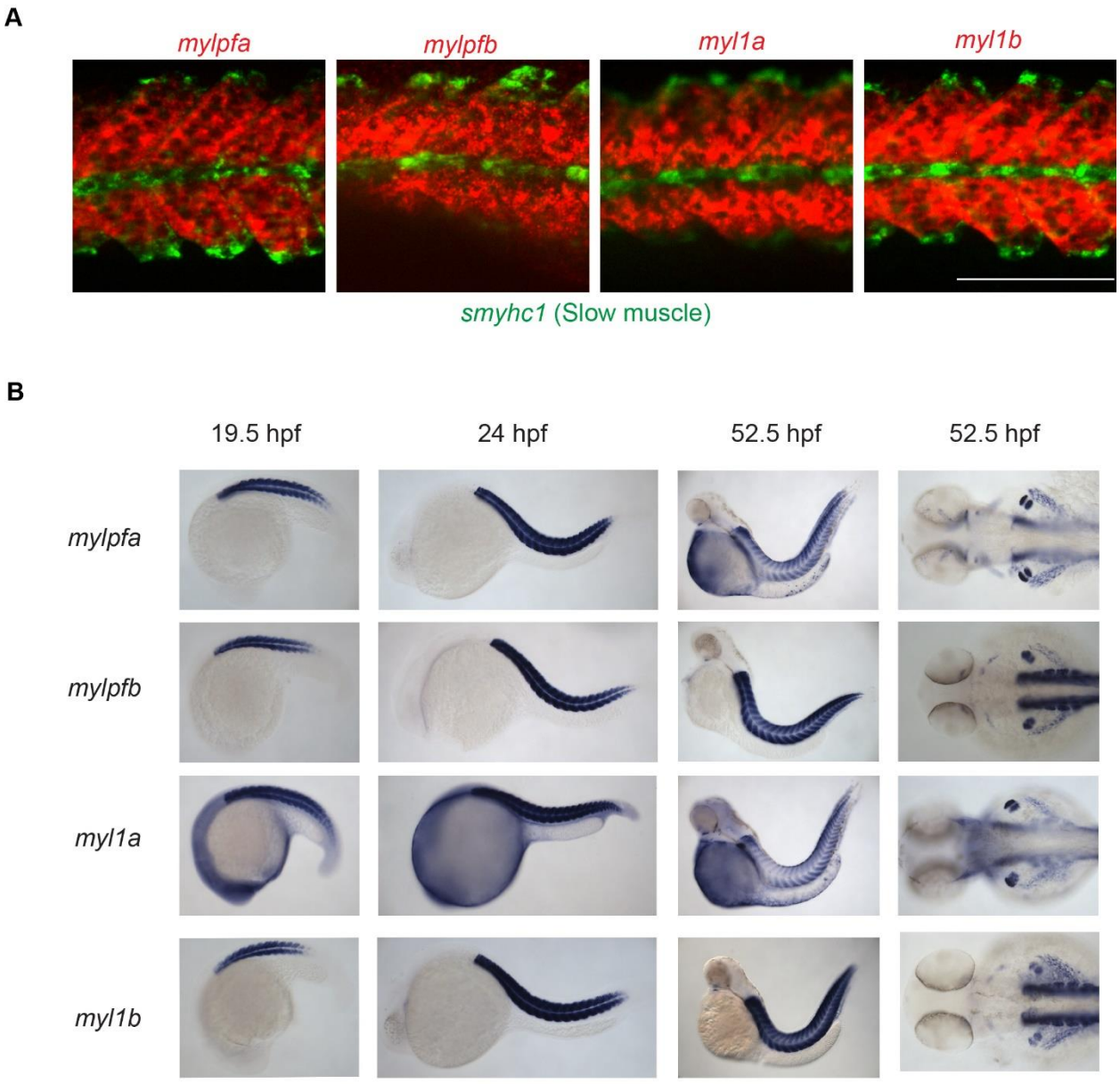

Figure 3. The four Myosin light chains exhibit similar fast muscle-specific RNA expression patterns.

(A) Confocal section of embryos labeled with probe to *smyhc1* as a slow muscle marker in green with one of each of the four Myosin light chain genes marked in red. Scalebar: 100 microns **(B)** Single RNA in situs of the four fast muscle specific Myosin light chain genes show fast muscle specific expression in the trunk beginning at 19.5 hpf that continues on through 52.5 hpf. Additionally, the fast muscle-specific hypaxial and pectoral fin muscles express all four of the Myosin light chain genes at 52.5 hpf.

Mutations in four Myosin light chain genes reveal Mylpfa as key for muscle organization

To test what the roles of the four Myosin light chains may be, I worked in collaboration with other members of the Amacher lab to mutate and identify lines carrying mutations in the four fast specific skeletal Myosin light chains using CRISPR/Cas9 mutagenesis. Our mutants cause an early frameshift mutation, likely truncating the proteins midway through the first EF Hand domain that binds the Myosin light chain to Myosin heavy chains. So, these mutations likely cause strong losses in gene function or are null. Examination of swimming behaviors in the four mutants revealed that *mylpfa*$^{-/-}$ mutants have severe defects. Thus, I have focused on the *mylpfa*$^{-/-}$ mutants for further characterization. The RLC have very similar amino acid sequences (**Figure 4A**), identical at 159 out of 170 sites, (94.1%). Thus, functional differences between the two genes is not likely caused by sequence differences. To test for differences in mutant phenotypes, I screened muscle organization in these mutants using the polarized light effect known as birefringence. *mylpfb*$^{-/-}$ homozygous mutants have normal birefringence. In contrast, *mylpfa* homozygous mutants have reduced birefringence (**Figure 4B**). Only *mylpfa*$^{-/-}$ mutants exhibit a consistent reduction in birefringence, suggesting that *mylpfa* is the key Myosin light chain gene for sarcomere formation.

Zebrafish express *mylpfa* at higher levels than the other Myosin light chains

These severe birefringence defects seen in the *mylpfa*$^{-/-}$ mutants are largely absent in *mylpfb*$^{-/-}$. To explain why *mylpfa* may be the critical Myosin light chain gene, I examined RNA seq data from another Amacher lab member, Pooja Gangras, to see if there was a difference in the *mylpfa* RNA expression level compared to that of *mylpfb*. From this data, I found that *mylpfa* expression is higher than its duplicate, *mylpfb* (**Figure 4C**). Both Essential light chain mutants (*myl1a* and *myl1b*) appear to have normal birefringent character. I did detect moderate swimming defects in *myl1a* mutants. Based on similar analysis of RNA seq data from Pooja Gangras, *myl1a* and *myl1b* are expressed at similar levels to one another, though at much lower

levels than *mylpfa.* I also confirmed this expression data using an online resource of RNA expression patterns in zebrafish (The European Bioinformatics Institute Expression Atlas). The online resource uses the alternative names for the Essential light chains: *myl1a* is referred to as *myl1* and *myl1b* is referred to as *mylz3.* Perhaps we do not see severe defects in the ELC mutants because either ELC gene can suffice for sarcomere organization and muscle function. However, since *myl1a* and *myl1b* bind to different locations on the neck of the Myosin heavy chain than the RLCs, it is unlikely that they can compensate for a loss of *mylpfa* in the *mylpfa*$^{-/-}$ mutants. Therefore, higher RNA expression levels of *mylpfa* when compared to *mylpfb* could explain the critical role of *mylpfa* in muscle organization and function.

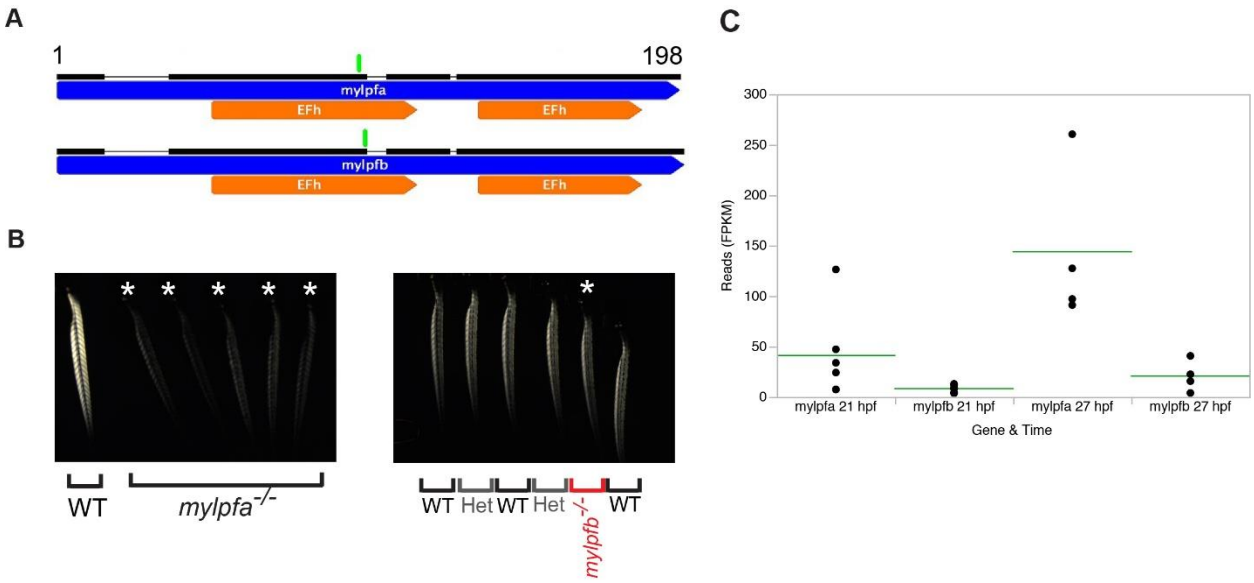

Figure 4. *mylpfa* is the key Regulatory light chain gene in fast muscle

(A) Protein alignments showing the two Regulatory Myosin light chains, Mylpfa and Mylpfb, and where they are truncated in mutants (green oval). Both mutants truncate in the first EF Hand domain (orange), which connects light chain proteins to Myosin heavy chains. **(B)** Muscle birefringence is bright in wild-type embryos (left most embryo) but dimmer in *mylpfa* mutants (asterisk). Mutants for *mylpfb* are indistinguishable from their wild-type siblings. **(C)** Graph of RNA-Seq data showing the number of fragments to the gene of interest (either *mylpfa* or *mylpfb*) per million mapped reads in wild-type at 21 hpf and 27 hpf. Individual points plotted come from different biological replicates.

***mylpfa* mutants have impaired swimming and immotile pec fins**

Sarcomeres are the basic contractile unit of muscle cells. Knowing this, I screened the mutant lines for muscle weakness by assaying their swimming. As expected based on their normal muscle organization as assayed by birefringence, *mylpfb*$^{-/-}$ mutant swimming patterns were indistinguishable from their wild-type and heterozygous siblings. In *mylpfa*$^{-/-}$ mutants, which have a severe reduction in birefringence and thus severe loss of muscle organization, I observe a strong swimming defect when compared to their wild-type siblings or to the other Myosin light chain mutants. Compared to their wild-type siblings, *mylpfa*$^{-/-}$ mutants swim in an abnormal manner: they swim more slowly, are slower to respond to mechanical probing, and cannot hold themselves upright for very long. *mylpfa*$^{-/-}$ mutants also have immotile pectoral fins, which are pure fast muscle. These *mylpfa*$^{-/-}$ specific swimming defects suggest that *mylpfa* is the critical Myosin light chain gene expressed in zebrafish fast muscle and is consistent with the finding that *mylpfa* expression is at a higher level than that of *mylpfb.*

***mylpfa* mutants have reduced skeletal muscle contractile strength**

To quantitatively test how loss of *mylpfa* affects muscle strength, I worked with Brit Martin in the Janssen lab to measure the force of muscle contraction after electrostimulation. We measured the contractile strength of wild-type siblings, *mylpfa*$^{+/-}$ heterozygotes, and *mylpfa*$^{-/-}$ mutants (**Figure 5A**). A current of various frequencies passed over the body of the zebrafish induces muscle contraction. The resulting force the fish exerts when the current induces its body to contract is then recorded (Martin et al., 2015). At 72 hpf, the homozygous *mylpfa*$^{-/-}$ mutant embryos had a significant reduction in contractile strength compared to both their heterozygous and homozygous wild-type siblings at all frequencies. A reduction in muscle area cannot explain this reduction in contractile strength, as *mylpfa*$^{-/-}$ mutants have similar cross-sectional muscle area than their wild-type siblings (**Figure 5B**). *mylpfa*$^{+/-}$ heterozygotes are not significantly different than the wild-type siblings (**Figure 5C**). Additionally, the *mylpfa*$^{-/-}$ embryo

myotome takes longer to reach peak contractile strength (**Figure 5D**) and is slower to relax (**Figure 5E**). This pattern of slower to reach peak force and to relax afterwards is characteristic of slow muscles, thus I hypothesize that the contractile strength of the *mylpfa*$^{-/-}$ mutants are mostly from the contraction of slow muscles. The *mylpfa*$^{-/-}$ mutant swimming defects we observe are significantly different from their wild-type and heterozygous siblings, potentially due to defective Myosin-Actin ratcheting.

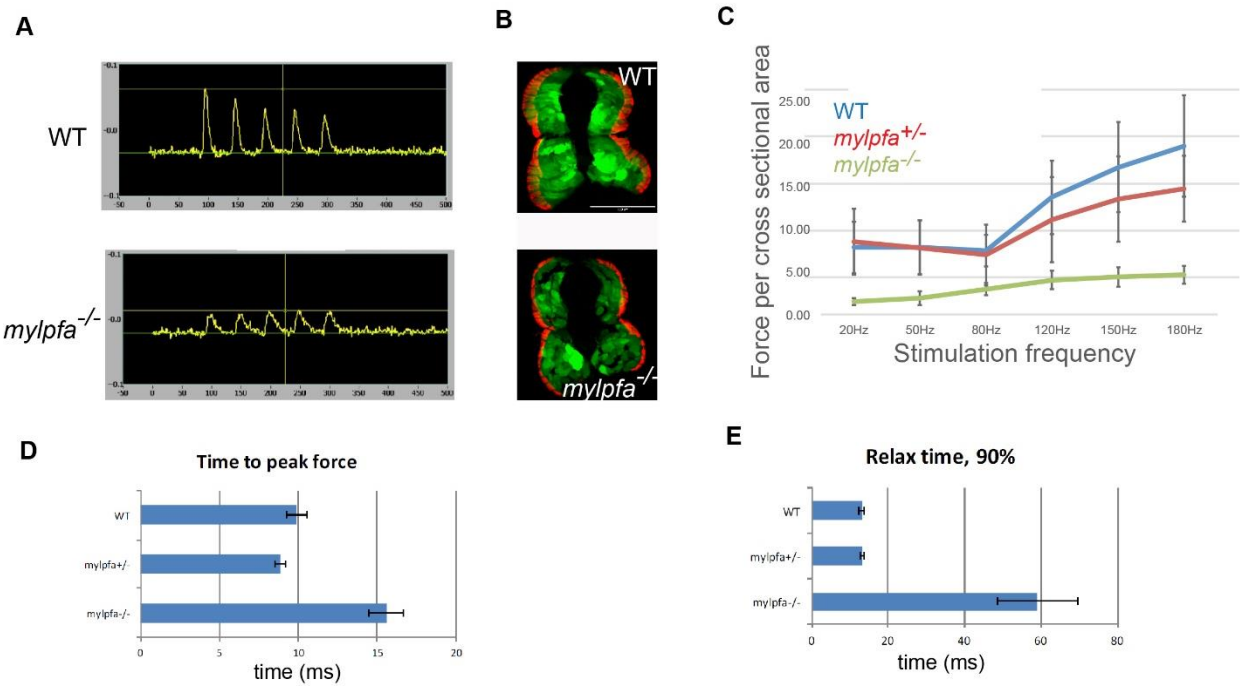

Figure 5. *mylpfa* is required for fast muscle contraction.
(A) Graphs showing contractile force outputs of wild-type and *mylpfa*$^{-/-}$ mutants at 3 dpf when electro-stimulated by 20 Hz. **(B)** Confocal image of a cross section of 3 dpf wild-type and *mylpfa*$^{-/-}$ mutant embryos expressing transgenes to mark fast (green) and slow (red) muscles. Scalebar: 100 microns **(C)** Graph of the contractile force of wild-type (blue), *mylpfa*$^{+/-}$ heterozygotes (red), and *mylpfa*$^{-/-}$ mutants (green) over various stimulation frequencies. **(D)** Bar graph depicting the time for wild-type, *mylpfa*$^{+/-}$ heterozygotes, and *mylpfa*$^{-/-}$ mutants to reach peak force and **(E)** the time to relax 90% from this peak force.

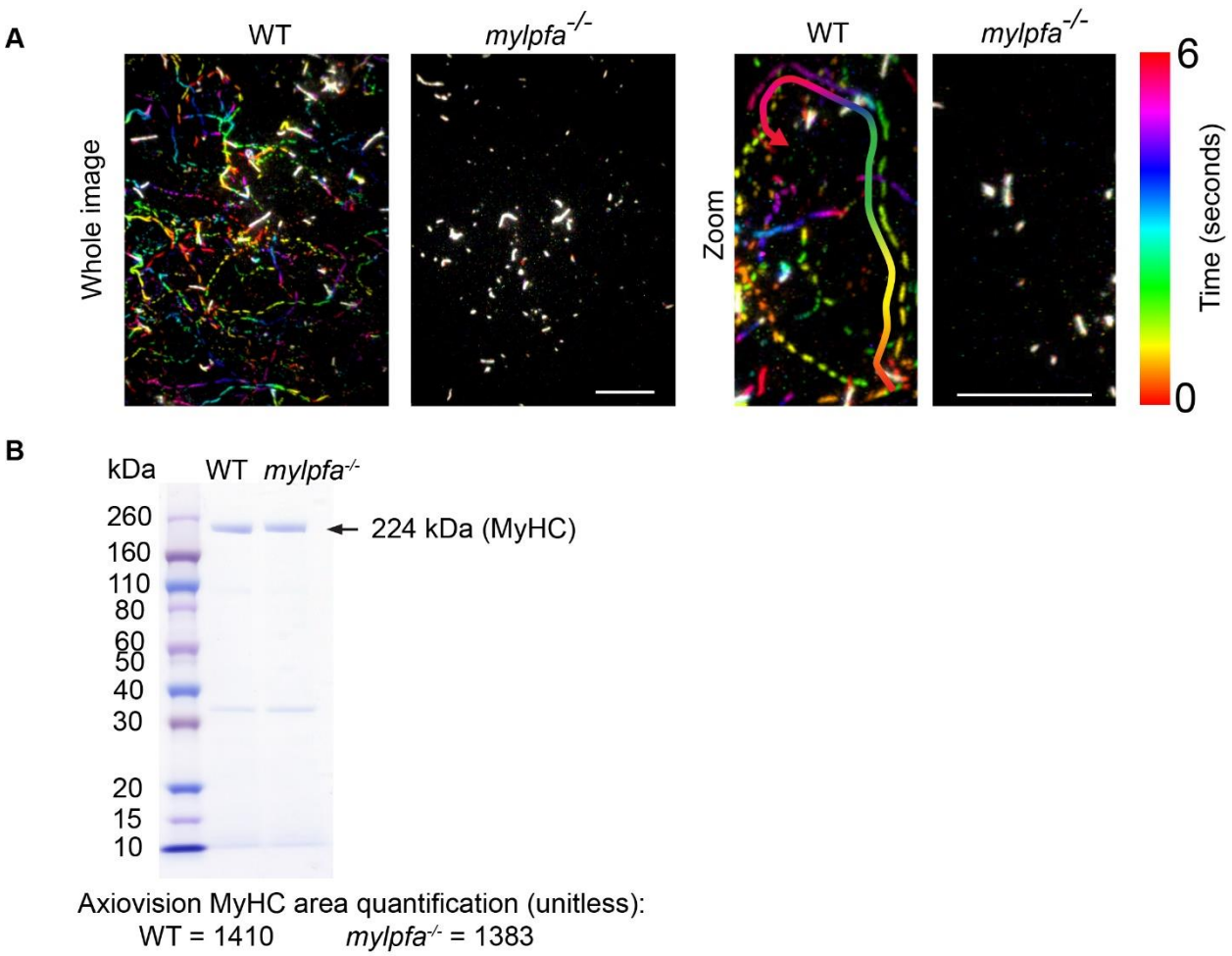

Figure 6. *mylpfa* mutants lack *in vitro* Myosin heavy chain activity
(A) Tracks of fluorescently labeled Actin filaments over time as they are moved by extracts from either wild-type of *mylpfa*$^{-/-}$ mutants. Filaments are tracked over 6 seconds using ImageJ and their location marked from time 0 (red) to 6 seconds (fuchsia/red). Scalebar: 10 microns **(B)** SDS gel of extracts enriched for Myosins from 3 dpf wild-type and *mylpfa*$^{-/-}$ mutant embryos. We quantified the area of the Myosin heavy chain band using Axiovision (unitless). The wild-type band has an area of 1410 and *mylpfa*$^{-/-}$ mutant band has an area of 1383.

Supplemental Movie 1
https://drive.google.com/open?id=18dDnzFlM7lt4J6Vg3P1ZLLmdw2n997Du
Recording of fluorescently labeled Actin filaments on slide with 3 dpf wild-type Myosin extracts.

Supplemental Movie 2
https://drive.google.com/open?id=1xSr6ayDSoAuW5AEJbVFt-dUmu6QdjKMQ
Recording of fluorescently labeled Actin filaments on slide with 3 dpf *mylpfa*$^{-/-}$ mutant Myosin extracts.

***mylpfa* mutants lack *in vitro* Myosin heavy chain activity**

Since zebrafish muscle expresses *mylpfa* transcripts at a higher level than its duplicate, *mylpfb*, a mutation in the *mylpfa* gene is more severe than a mutation in *mylpfb*. If *mylpfa* and *mylpfb* have equivalent roles, then a mutation in *mylpfa* is more similar to a full loss of RLC. Previous research had shown that in vitro Myosin activity is reduced in the absence of the RLC (Lowey et al., 1993b). Based on this previous research on the loss of RLC on Myosin function as well as our in vivo results of muscle weakness, I tested the activity of Myosin extracted from *mylpfa*$^{-/-}$ mutants. In August 2017, I traveled to the University of Vermont to collaborate. Together, we extracted Myosins from 72 hpf wild-type and *mylpfa*$^{-/-}$ mutant embryos and measured their Actin-Myosin motility in vitro as described previously (Lin et al., 2018). The *mylpfa*$^{-/-}$ mutant extracts induced little to no Actin movement, a dramatic reduction compared to their wild-type siblings (**Figure 6A, Supplemental Movies 1 and 2**). Additionally, less total Actin is bound to the slide, suggesting that there are fewer Myosin heavy chains binding to the fluorescently labeled Actin. To ensure that a reduction in Myosin heavy chain protein doesn't explain the reduction in Actin binding and Actin, I measured the relative Myosin heavy chain levels in wild-type versus *mylpfa*$^{-/-}$ mutants. We saw no difference in the band intensity for the band size corresponding to Myosin heavy chain protein when we ran Myosin-enriched on an SDS-Page gel (**Figure 6B**). Additionally, antibody labeling of Myosin heavy chain on sections of *mylpfa*$^{-/-}$ mutants does not appear significantly reduced when compared to their wild-type siblings (**Figure 7D**). Thus, I conclude that a loss of Mylpfa protein and not a reduction in Myosin heavy chain explains the reduction in Myosin heavy chain activity in vitro.

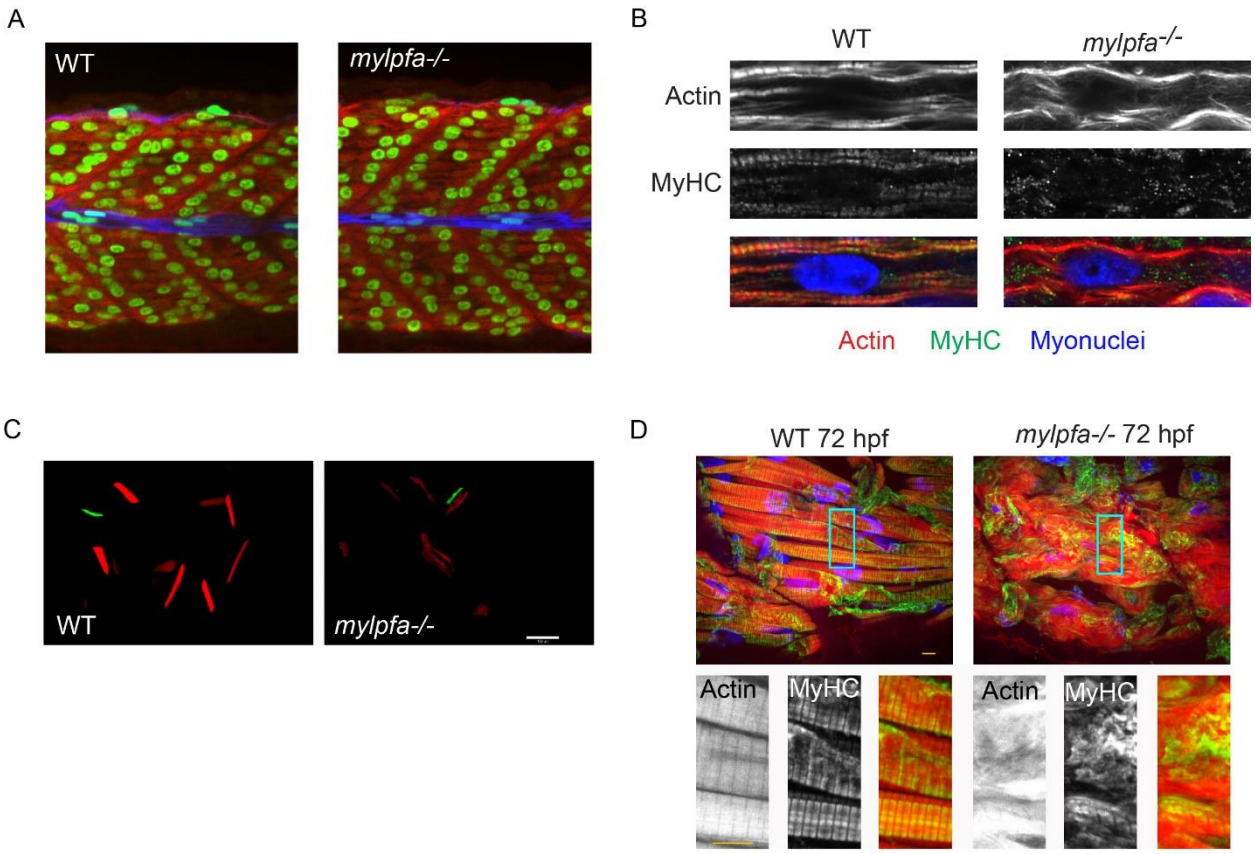

Figure 7. *mylpfa*$^{-/-}$ mutants have sarcomeric organization defects but relatively normal overall muscle organization.

(A) Confocal cross section of 26 hpf embryos labeled with antibodies for fast muscle (red), slow muscle (blue), and nuclei (green) markers show normal muscle type separation and myotome organization in *mylpfa*$^{-/-}$ mutants. **(B)** High magnification in confocal microscopy of 26 hpf embryos labeled for Actin (red), Myosin heavy chain (green) and myonuclei (blue) show poor co-localization between Myosin heavy chain and Actin in *mylpfa*$^{-/-}$ mutants. **(C)** Confocal images of fast (red) and slow (green) muscle fibers extracted from *mylpfa*$^{-/-}$ mutants. Scalebar: 100 microns **(D)** Confocal images of sectioned 3 dpf embryos labeled with Actin (red) and Myosin heavy chain (green). *mylpfa*$^{-/-}$ mutants have both aggregates of Myosin heavy chain and patches of sarcomere organization. Scalebar: 5 microns

Mylpfa mutants have severe defects in sarcomere development

The Myosin heavy chains are present at wild-type levels in the *mylpfa*$^{-/-}$ mutants; however, the Myosin extracts bind and move fewer Actin filaments. I wanted to test in vivo whether the Myosin heavy chains are able to interact with Actin filaments. Additionally, I wanted

to examine the muscle structure of the *mylpfa*$^{-/-}$ mutants since the reduction in birefringence suggests disorganization. At 26 hpf, overall muscle fiber organization appears normal in *mylpfa*$^{-/-}$ mutant skeletal muscles (**Figure 7A**). Thus, slow and fast muscle fibers still develop and separate in *mylpfa*$^{-/-}$ mutants. To look more closely at the sarcomeric organization of the skeletal muscle, I observed the localization of the Myosin heavy chains in relation to the Actin using antibody labeling. In 26 hpf wild-type embryos, there is alternating labeling of Actin and Myosin, indicating that Myosin heavy chains and Actin are interacting with one another. In contrast, Myosin heavy chains and Actin do not display proper sarcomeric organization in 26 hpf *mylpfa*$^{-/-}$ mutants. Actin myofibrils are present in *mylpfa*$^{-/-}$ mutants, but they do not associate with Myosin heavy chain (**Figure 7B**). By 72 hpf, the fast muscle fibers themselves appear to have an abnormal morphology. It is difficult to observe exact morphology of individual fibers in the whole zebrafish embryo, so we isolated fast muscle fibers from wild-type and *mylpfa*$^{-/-}$ mutant embryos at 72 hpf. Isolated mutant fibers were more fragile than the wild-type fibers and often balled up or broke in transfer (**Figure 7C**). To examine both Actin and Myosin, I sectioned the 72 hpf embryos and labeled the sarcomeric structure. In *mylpfa*$^{-/-}$ mutants there are patches of sarcomeric organization, but most of the muscle fiber remains disorganized (**Figure 7D**). By 72 hpf, much of the Myosin heavy chain appears to aggregate together instead of lining up with the actin filaments. Even within a single muscle fiber there may be small portions of sarcomere organization adjacent to globs of Myosin heavy chain aggregates. The aggregation of the Myosin heavy chain may explain why the Myosin extracts for the in vitro Actin activity assay was unable to bind to Actin at this developmental stage. Alternatively, the Myosin may never have been able to bind Actin in the absence of *mylpfa*$^{-/-}$. The disorganization of sarcomeric structure correlates well with the reduction of birefringence and muscle weakness seen in *mylpfa*$^{-/-}$ mutants.

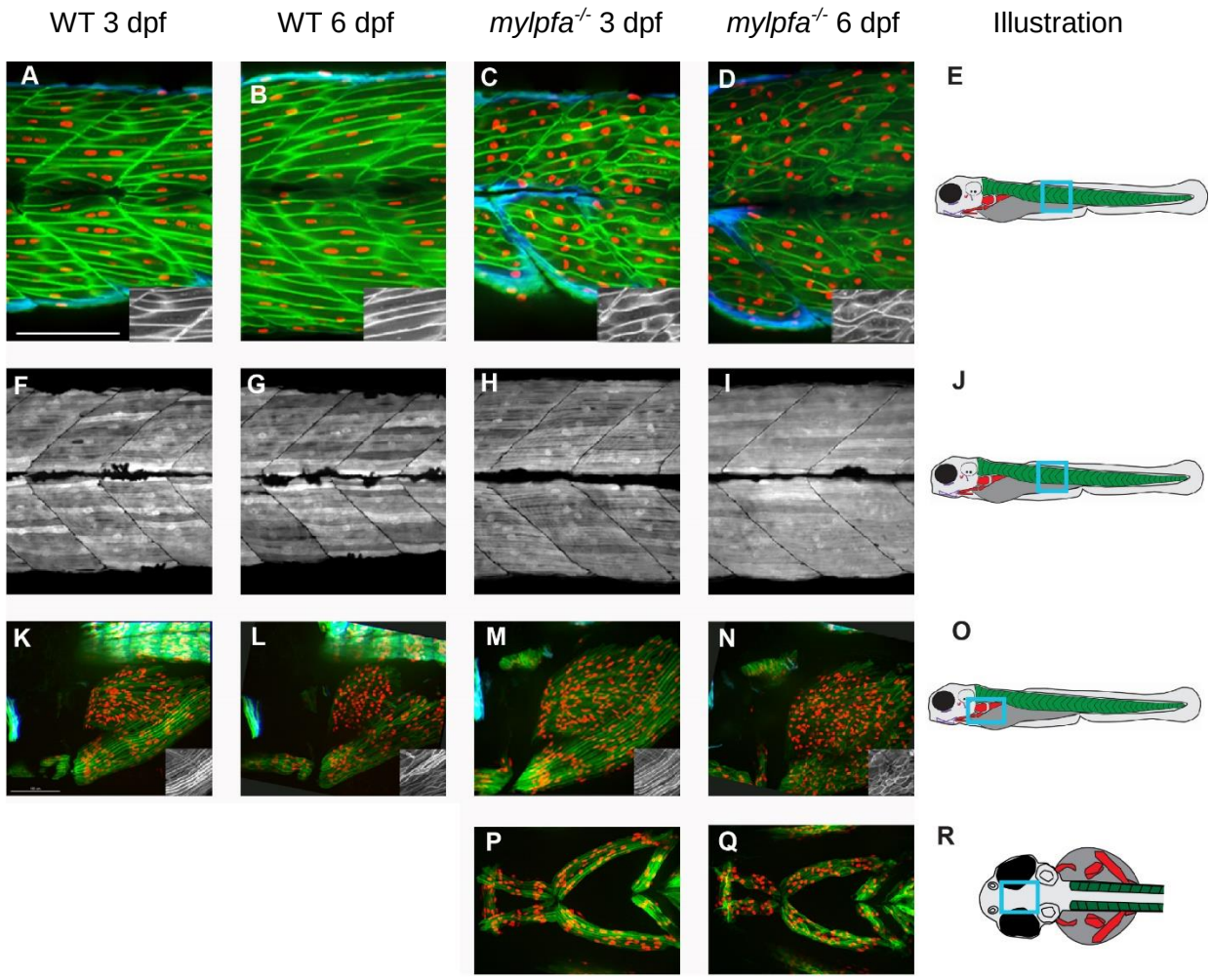

Figure 8. Fast muscles in *mylpfa*$^{-/-}$ mutants degenerate between 3 and 6 dpf.

Confocal section of embryos expressing transgenes marking fast muscle (green), slow muscle (blue), and nuclei (red). **(A, B)** Whereas wild-type muscle appears stable over time, **(C, D)** *mylpfa*$^{-/-}$ trunk muscles degenerate between 3 dpf and 6 dpf**. (F-I)** Projections of slow muscle marker *smyhc1:GFP* show muscles show that slow muscle is not overtly affected by loss of *mylpfa*. **(K-Q)** Other *mylpfa* expressing muscle groups such as the hypaxial and pectoral fin muscles **(K-N)** and the facial muscles **(P, Q)** also degenerate in *mylpfa*$^{-/-}$ mutants but not their wild-type siblings. **(E, J, O, R)** Images are of the region represented by the blue box on the illustrations of 3 dpf embryos**.** Scalebar: 100 microns

Fast muscles in *mylpfa*$^{-/-}$ mutants degenerate between 72 hpf and 96 hpf

Despite the severe lack of sarcomeric organization at 72 hpf, fast muscle fibers in the mutants are only slightly more irregularly shaped than in wild-type embryos. To test the effect of time and increased mechanical activity on the *mylpfa*$^{-/-}$ mutant muscle, I followed the muscle fibers over time using transgenic markers of fast and slow muscles. Between 72 and 96 hpf, fast muscle fibers in the trunk rapidly degenerate into small islands of cells that have zero to two nuclei per cell (**Figure 8A-E**). The slow muscles, however, remain unaffected during this time (**Figure 8F-J**). Other groups of fast muscle fibers in the zebrafish such as the fin and hypaxial muscles (**Figure 8K-O**) and the facial muscles (**Figure 8P-R**) also exhibit this pattern of degeneration. In *mylpfa*$^{-/-}$ mutants, but not in their wild-type and heterozygous siblings, there is a significant increase in the number of breaks and small islands of cells (**Figure 9, Supplemental Movie 3**). Thus, in the absence of *mylpfa*, muscle fibers form, but lack the sarcomeric organization required for maintenance of muscle integrity.

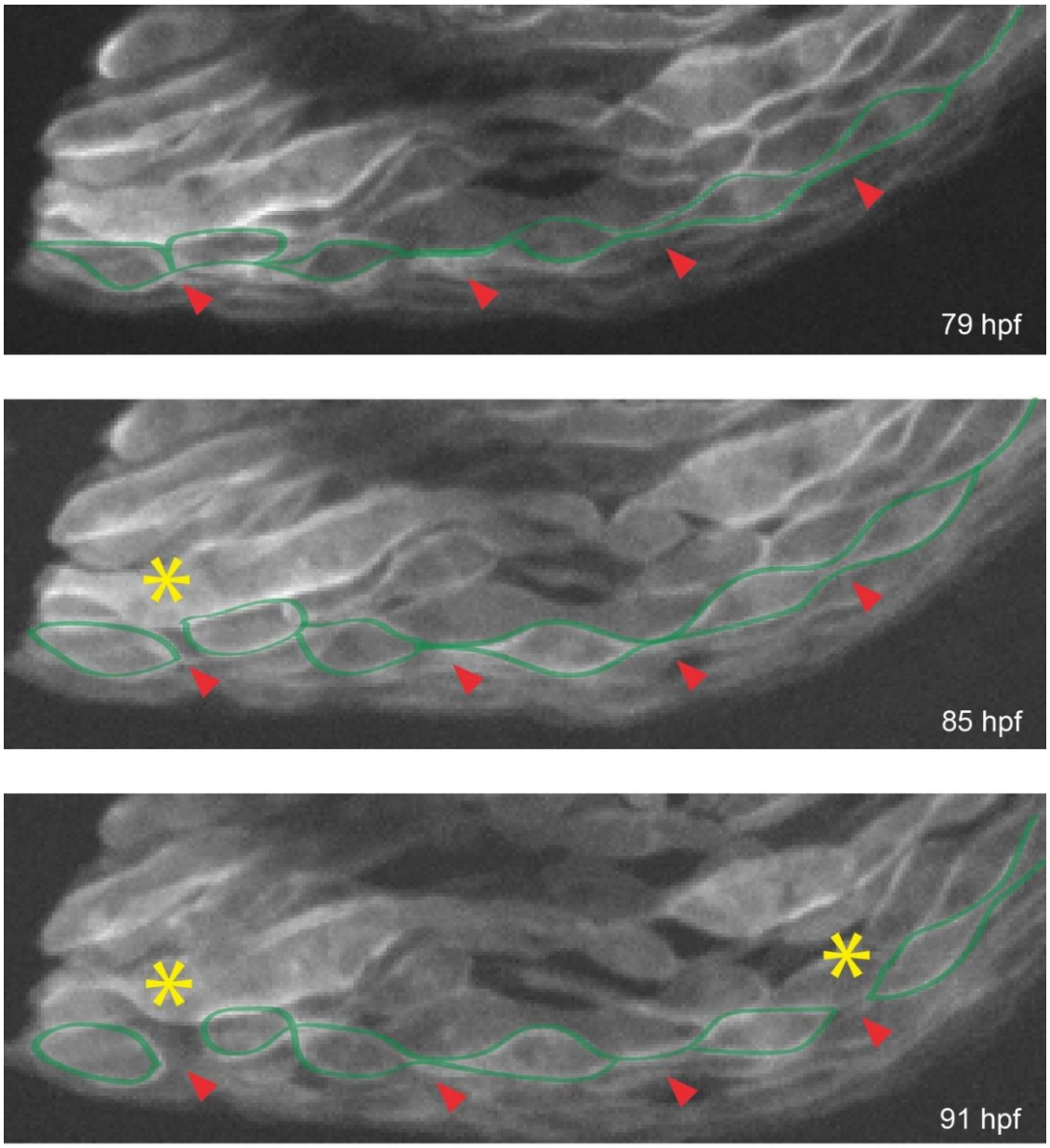

Figure 9. Fast muscles break along the length of myofibers in *mylpfa*$^{-/-}$ mutants, forming small rounded cell 'islands'

Still images from timelapse of the hypaxial muscle of a *mylpfa*$^{-/-}$ mutant from 79 hpf to 91 hpf. The membrane of a single myofiber was pseudo colored green. Red arrow heads indicate points of pinching of the myofiber and yellow asterisks indicate breaks in the myofiber.

Supplemental Movie 3

https://drive.google.com/open?id=1goOyGVLW8NOt0PNQB7KzE2sGD6FYtHCU

Timelapse of *mylpfa*$^{-/-}$ mutant from 79 hpf to 94 hpf with images taken every 7 minutes.

Discussion

Despite similar amino acid sequences and spatial expression patterns, I identified *mylpfa* as the key Regulatory myosin light chain gene for muscle integrity and function. *mylpfa*$^{-/-}$ mutants exhibit severe sarcomeric organization defects beginning as early as 26 hpf. Wild-type embryos at 26 hpf have sarcomeric organization that resembles the nascent myofibrils described in the three-step model of myofibrillogenesis (Sanger et al., 2017). In contrast, in *mylpfa*$^{-/-}$ mutants, Actin filaments span the myofiber but are less organized than in wild-type siblings at the same developmental stage. If muscle Myosin does not integrate into the organized Actin filaments in what would be the second step of myofibrillogenesis, as the non-muscle myosin degrades or leaves the pre-sarcomeric structure, the Actin may diffuse throughout the myofibril. Thus, a lack of functional Myosin heavy chains could lead to disorganization of Actin filaments. As more of the muscle Myosin should replace non-muscle Myosin, Actin structure in *mylpfa*$^{-/-}$ mutants disperses further, losing its previous organization. If Myosin heavy chain association with Actin filaments require *mylpfa,* this could explain the failure in the second step of myofibrillogenesis and the lack of sarcomeric organization in *mylpfa*$^{-/-}$ mutants. My data suggest that maintenance of Actin filamentous structure throughout the entirety of myofibril development requires the association of muscle Myosin heavy chains and Actin.

In *Drosophila*, micro-contractions further form sarcomeric structure by aligning the other forming sarcomeres together during the maturation of the myofibril. In wild-type zebrafish, sarcomeric structure becomes more robust over time. In *mylpfa*$^{-/-}$ mutants, however, there are only patches of sarcomeric structure by 72 hpf, perhaps due to the other RLC *mylpfb.* To test whether *mylpfb* partially compensates for loss of *mylpfa*, I will examine *mylpfa*$^{-/-}$; *mylpfb*$^{-/-}$ double mutants for the small patches of sarcomere organization. I hypothesize that in these double mutants, I will see no patches of sarcomeric organization even at 72 hpf. The patches in the

single *mylpfa*$^{-/-}$ mutants may still be capable of localized contraction and align sarcomeres together. I could test whether it is levels of RLC that is important as opposed to a difference in *mylpfa* or *mylpfb* function by injecting embryos with *mylpfb* mRNA to overexpress *mylpfb.* If this is sufficient to rescue the *mylpfa*$^{-/-}$ mutants then the phenotype we observe is caused by insufficient levels of RLC and not a loss of *mylpfa* in particular. The amount of *mylpfb* in *mylpfa*$^{-/-}$ mutants is likely not enough to compensate for an entire myofibril, thus these sarcomeric structures remain localized. Over time, as these patches of sarcomeres mature, they strengthen and may be responsible for pulling in on the fiber, collapsing it. Thus, the patches of sarcomere structure may be responsible for the degeneration of *mylpfa*$^{-/-}$ mutant muscle. I propose a model in which a failure of proper sarcomere organization leads to muscle fiber collapse in areas lacking sarcomeres. Patches of sarcomeres that form further pull on the myofiber, breaking the muscle off into smaller mononucleated cell islands (**Figure 10**). The degenerated trunk fast muscles in zebrafish appear similar to the phenotype of the *Mylpf*$^{-/-}$ mutant newborn mouse (Wang et al., 2007). Perhaps the mouse *Mylpf*$^{-/-}$ mutant also has sarcomere organization and myofibrillogenesis that led to the muscle degeneration. To directly visualize how sarcomere structure corresponds to muscle 'islands' in our *mylpfa*$^{-/-}$ mutants, we could perform a time lapse using our muscle membrane marker (*mylpfa: lyn-Cyan*) and a sarcomere marker (LifeAct-mCherry mRNA) in *mylpfa*$^{-/-}$ mutants during degeneration. My degeneration hypothesis supports that micro-contractions of the patches of sarcomere cause muscle degeneration. Thus, I hypothesize that myofibers will break along the myofiber adjacent to functional patches of sarcomere structure in *mylpfa*$^{-/-}$ mutants. Additionally, if the patches of sarcomere are destructive for the myofiber, if we were to inhibit muscle contraction via Myosin inhibitors, the muscles would not degenerate.

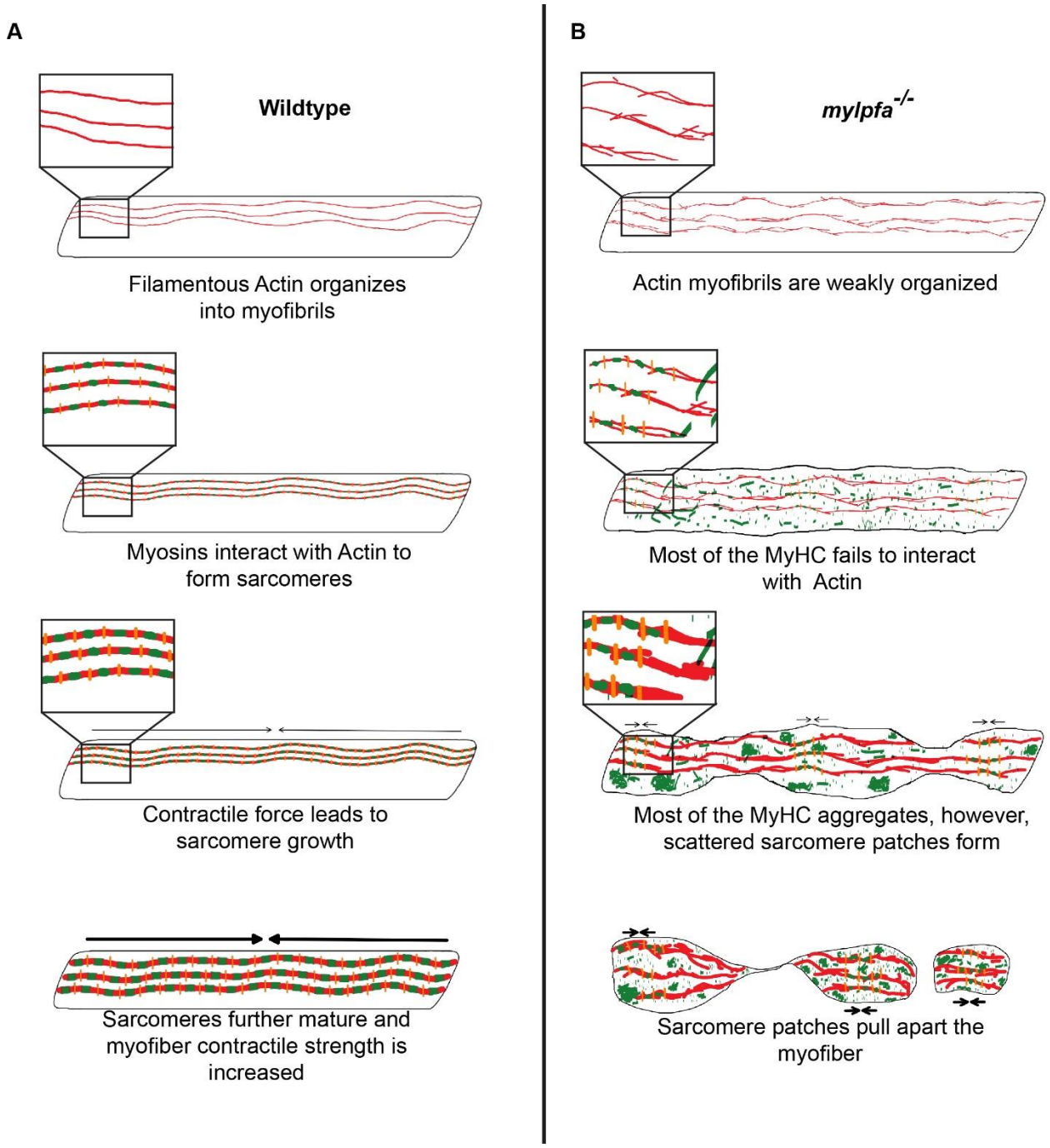

Figure 10. Actin-Myosin interactions are required for sarcomere assembly and muscle integrity.

(A) Model for wild-type sarcomere organization in myofibers. **(B)** Illustration of my model for the failure of sarcomere organization in *mylpfa*$^{-/-}$ mutants and how this leads to degeneration of myofibers.

Another possible explanation could be that the small patches of sarcomere structure are not destructive in the *mylpfa*$^{-/-}$ mutants but are constructive in maintaining the shape of the smaller muscle islands. There is not enough sarcomere organization to maintain the shape of the entire myofibril; however, there is enough to maintain the integrity of the smaller islands. Thus, instead of the sarcomeres pulling the fiber apart, the fibers are collapsing in on the areas of the greatest absence of sarcomere structure. If these sarcomere patches in *mylpfa*$^{-/-}$ mutants are indeed due to the presence of *mylpfb,* in examining the *mylpfa*$^{-/-}$*; mylpfb*$^{-/-}$ double mutants, we should see no sarcomere organization throughout the myofibril. If the patches of sarcomeres in *mylpfa*$^{-/-}$ mutants are constructive as opposed to destructive, in double mutants I should still see muscle degeneration, or perhaps degeneration that occurs sooner or with more breaks across the myofiber. *Mylpf*$^{-/-}$ mouse mutants do not have a duplicate of the RLC gene and still appear to be similar to the *mylpfa*$^{-/-}$ mutants, supporting the possibility of degeneration in *mylpfa*$^{-/-}$ mutants is due to the lack of the majority of sarcomere organization.

Myosin heavy chains in *mylpfa*$^{-/-}$ mutants not only lack association with Actin, but also appear to aggregate by 72 hpf. In the absence of *mylpfa,* the Myosin heavy chains are likely unstable by themselves, leading to aggregates in the absence of Actin association. This aggregation of Myosin heavy chains could also explain why the in vitro assay of Myosin heavy chains activity was lower in *mylpfa*$^{-/-}$ mutants. The Myosins may not be able to ratchet Actin without *mylpfa* and may not be available to bind to the Actin because much of the Myosin has aggregated together. I will use Transmission Electron Microscopy to further visualize both the small patches of sarcomere structure and the Myosin heavy chain aggregates. Aggregates of sarcomeric proteins such as the Myosins have been associated with a group of muscular dystrophies known as myofibrillar myopathies (Sharma and Goebel, 2005). Thus, *mylpfa*$^{-/-}$ mutants may provide a model organism for studying such protein aggregate myopathies.

Myosin heavy and light chains have been shown to be linked to several other disorders in human skeletal and cardiac muscles. Mutations in the slow muscle and cardiac myosin light chains MYL2 and MYL3 lead to skeletal and cardiac myopathies (Hwang and Sykes, 2015). Mutations in myosin heavy chains, another component of the sarcomere, have been linked to human diseases, including muscle degenerative diseases. Mutations in the slow myosin heavy chain MYH7 in humans that alter the protein's confirmation are linked to Laing muscular myopathy, a form of muscular dystrophy (Meredith et al., 2004). Defects in sarcomeric proteins like Myosins may also help explain patient variation in Duchenne Muscular Dystrophy. Evidence of such a link has been shown in dystrophy patients with a null polymorphism in ACTN3, which normally encodes another sarcomeric protein, α-Actinin-3 (Hogarth et al., 2017). By understanding the roles of the Myosin light chains, such as Mylpfa, researchers can better understand and treat disorders that arise from or are modified by mutations in these genes in the future.

Materials and Methods

Fish maintenance, husbandry, and strains.

Fish were raised and maintained under standard conditions and staged as described previously (Kimmel et al., 1995) Westerfield, 2007). I used the following transgenic lines to study the muscle structure: *tg(smyhc1:EGFP)i104* referred to as *smyhc1:GFP* (Elworthy et al., 2008), *tg(myog-Has.HIST1H2BJ:mRFP)fb121* referred to as *myogenin:H2B-mRFP* (Tang et al., 2016), *tg(mylpfa:LY-CFP)fb122* referred to as *mylpfa:lyn-cyan* (Tang et al., 2016), and *tg(mylpfa:mCherry)cz3327)* referred to as *mylpfa:mCherry* (Ignatius et al., 2012). *smyhc1:GFP* was provided by Phil Ingham's lab. *mylpfa:H2b-mRFP*, *mylpfa:mCherry*, and *mylpfa:lyn-Cyan* were provided by David Langenau's lab. Mutant lines of the four Myosin light chain genes were constructed as described below.

CRISPR mutagenesis

CRISPR mutagenesis and mutant recovery was performed as described previously (Talbot and Amacher 2014). Jared Talbot designed and injected CRISPR/Cas9 into embryos to generate mutants in the four myosin light chain genes. We used guide oligo targeting sequence GGTGAAGTTGATTGGGCCGC to mutate *mylpfa* and screened for founders using primers TCTCTACAGGCCAGCTGAATG and ACCCTTCAACTTCTCTCCGAAC. To mutate *mylpfb*, we used guide RNA to target sequence GGAAAACAGTAAAGTTGATG and screened for potential founders using HRMA with primers GCAACAATGGGTCAGCTAAATG and GGTAAGTGAAGATTTGGACAACTC. *myl1a* was mutated using guide RNA to CGATTTCACCCAGGACCAGA and potential founders were identified using primers CCTGCAGCTCGATTTC and TGGAAGATTGTGTCAAAGG. We used guide RNA to target sequence GGGTCAGAACCCCACCAACA to mutate *myl1b* and identified founders using primers AGAGTTGGTGACAGCAAGGTTG and ATGGTCTTACCGTCAGCAGATG. Pooja Gangras identified founders and established the line of fish carrying null mutations in *myl1b* as

well as conducted initial characterization of these mutants. Sarah Shepherd identified founders for *myl1a* and identified F1 fish carrying null mutations for *mylpfb* that I had identified the parental generation. I performed all other founder identification and allele sequencing. *mylpfa^oz30* has a 20 bp deletion without further substitutions that frameshifts after amino acid 76 of 169 and introduces 12 aberrant amino acids before termination. *mylpfb^oz39* has a 5 bp deletion that frameshifts after amino acid 78 of 171 and introduces 9 aberrant amino acids before reaching a stop codon. *myl1b* allele is still pending. *myl1b^oz14* is a 2 bp deletion without further substitutions leading to a frameshift after amino acid 46 of 151 and introduces 3 aberrant amino acids before reaching a stop codon. To genotype each of the Myosin light chain mutants, I use the same primers to identify founders as I used to identify founders of above mutants. Due to the large 20 bp deletion, *mylpfa* PCR product could be run on a 3% agarose gel to identify mutants. *mylpfb* PCR products must first be digested by *BccI* and then run on a 2% gel. The mutated allele for *myl1a* has yet to be confirmed by homozygous mutant analysis so as of now they are genotyped by HRMA. Finally, *myl1b* is genotyped by digesting PCR products with *BslI* with an extra cut site introduced in the *myl1b* mutants.

Tissue labeling

Antibodies and stains used for tissue labeling are as follows: Rbfox1l (recognized with Rabbi-405, conc. 1:500), A4.1025 (recognized with IgG2a-633, conc. 1:100), A4.1025 (recognized with IgG2a-488, conc. 1:100), F310 (recognized with IgG1-546, conc. 1:1000), and Phalloidin-546 (conc. 1:20 at 26 hpf, 1:50 at 3 dpf sections). Embryos were fixed in 4% PFA for two hours at room temperature or overnight at 4 degrees. Embryos were then washed out of fixative into 1X Phosphate Buffered Saline Tween-20 (PBST). If embryos were 3 dpf, they were briefly treated with Proteinase K to make them more permeable to the antibodies. Embryos were then placed in K block (1XPBS, 0.5% TritonX-100, 4% NGS 2% NSS 1% DMSO) for at least two hours at room temperature. Primary antibodies were prepared in K block and were added to embryos, rocking at room temperature overnight. Embryos were then washed in PBST-B-N (1X PBS,

0.1% Tween-20, 2% BSA, and 5% NGS) once then in PBST-B (1X PBS, 0.1% Tween-20, 2% BSA) three times over an hour. Secondary antibodies are also prepared in K block and allowed to preabsorb for at least 20 minutes before being added to the fixed embryos. Embryos then rock at room temperature for four hours or overnight at 4 degrees, after which they are washed out of secondary antibodies and into PBST.

Tissue Labeling of sections

Zebrafish embryos were raised to 3 dpf and then sectioned on the Cryostat by Kimberly Hromowyk. Eight sections were placed on each slide and rinsed for 30 minutes in 1X PBS. Sections on the slide were then outlined using a DAKO pen. Tissue was then permeabilized using 0.5% Triton in 1X PBS for 10 minutes. Sections were washed in 1X PBS for 10 minutes before being washed in block (0.03 g/mL BSA in 1X PBS) for 20 minutes. Primary antibodies were made in block and added to the sections overnight at 4 degrees. Slides were then washed in 1X PBS 4 times over an hour. Sections were treated with 0.1% Triton/1X PBS for 10 minutes before secondary antibodies were added and left at 4 degrees overnight. Finally, slides were washed in 1X PBS for 2 hours and coverslips were added. Slides were then imaged an inverted Nikon TiE microscope with an Andor Revolution WD spinning disk confocal system.

Birefringence

Zebrafish embryos were characterized for the optical property of birefringence. 3 dpf embryos were anesthetized using tricaine and 10 embryos were transferred to a 1 mL glass bottom dish at a time. Two polarizing filters were placed on the light microscope and rotated 90 degrees to one another. Because muscle is birefringent, it rotates light between these filters making the muscle appear to light up Embryos were then sorted based on their birefringent characteristics and transferred to new plates.

mRNA in situ hybridization

Fluorescent mRNA in situ hybridization was performed as described (Talbot et al., 2010) and non-fluorescent RNA in situ hybridization used established protocols (Jowett, 1999), with slight

modifications as follows. Embryos were treated with 1µg/ml Proteinase K for 5 minutes (24 hpf embryos) or for 45 minutes (52.5 hpf embryos). For in situs of time points after 1 dpf, embryos were treated with 0.003% N-Phenylthiourea (PTU) beginning at 24 hpf to prevent pigment formation. The *mylpfa* and *smyhc1* probes have been previously described (von Hofsten et al., 2008; Xu et al., 2000). We also confirmed the *mylpfa* expression pattern using an independent probe that I generated. I also generated the probe to *mylpfb* that covers 408 bp of the coding region and the 3' UTR from cDNA using the primers AGTGGCCCCATCAACTTTACTG and AGCCCAAATGCCAACAAACC. I also generated the probe to *myl1a* that covers 723 bp of the coding and 3' UTR sequence using cDNA from the primers TCCACTCCCTGTGTCGTGTTCCTTC and GTGTCCCTTTCATCCGTTTCTGAGTTGG. Jared Talbot generated the *myl1b* probe that covers 403 bp of the 3' UTR from cDNA using the primers CGTCTAGGGAGTGGTGAAGAAG and ATGACTGTGTGAAAATTGGGATGG. Embryos were mounted for imaging as described in (Morrow et al., 2017).

RNA-seq

RNA-seq was conducted by Pooja Gangras. For RNA-seq, mRNA was harvested from 21 and 27 hpf wild-type embryos, then ligated to a homemade linker library and sequenced on an Illumina HighSeq2500. RNA-seq conclusions were confirmed using publicly available data from The European Bioinformatics Institute (EMBL-EBI) Expression Atlas (https://www.ebi.ac.uk/gxa/experiments/E-ERAD-475/Results)

In vitro Myosin functional assay

In vitro motility assay was performed by Amy Li from David Warshaw's lab using embryos that I de-yolked and then permeabilized using Trypsin. I transferred 3 dpf embryos sorted mutant or wild-type by swimming behavior and birefringence to a plate of 2 mL of protease solution (2.5 mg/mL Trypsin, 0.2% 0.5 EDTA, 10% 10X phosphate-buffered saline (PBS), sterile H20 to desired volume) with 0.1% tricaine solution for 7.5 minutes. 500 microliters of stop solution (25% fetal calf serum/fetal bovine serum, 0.5% 1M calcium chloride, 10% 10X PBS, 64.5% sterile

water) to the embryos. After 1 minute, embryos were transferred to a new plate of Ringer's solution (0.29% 1 M potassium chloride, 2.32% 5 M sodium chloride, 0.5% 1 M Hepes pH 7.2, 96.89% sterile water). Embryos were then placed in a flow cell and washed with buffer and salt solutions to extract Myosins as described in (Scheid et al., 2017). The Myosins stick to the surface of the flow cell and fluorescently labeled Actin is washed through the flow cell and is bound by the Myosin. The fluorescently labeled Actin filaments are then imaged over 6 seconds.

Muscle motility assay

Functional muscle motility assay was performed by Brit Martin as described in (Martin et al., 2015). Embryos were raised to 3 dpf and mutants were sorted by their swimming defects. Anesthetized embryo tails were hooked to a force transducer and their head affixed in place. Embryos were stimulated for 250 ms at 20, 50, 80, 120, 150, and 180 Hz. Embryos were left unstimulated for 2 minutes between stimulations. I then genotyped these embryos to confirm mutant genotype and sort between wild-type and heterozygous embryos.

Time lapse imaging

mylpfa$^{-/-}$ mutants carrying the transgenic lines *smyhc1*:*GFP*, *myogenin:H2B-mRFP,* and *mylpfa:lyn-cyan* were raised to 3 dpf and sorted positive for expressing all three transgenes and mutant swimming phenotype. Embryos were mounted in system water with 0.2% agarose (GeneMate E-3120-500) that was heated and then cooled to 42 degrees before adding tricaine to a concentration of 0.02%. Embryos were then imaged using an inverted Nikon TiE microscope with an Andor Revolution WD spinning disk confocal system and analyzed using Metamorph software. Imaged embryos were then raised to 6 dpf in normal system water to check for health. Finally, genotype was confirmed using PCR.

Muscle fiber isolation

Similar to the first steps of the in vitro Myosin functional assay, embryos were raised to 3 dpf and sorted by the mutant swimming phenotype and by the reduction in birefringent character. The embryos were then placed in Ringer's solution with 0.02% tricaine solution. Insect pokers

were used to remove the yolks of the embryos. Embryos were transferred to a new plate of ringers and placed on a horizontal shaker for 5 minutes. Embryos were then transferred to a plate of 2 mL of protease solution with 0.1% tricaine solution for 7.5 minutes. 500 microliters of stop solution to the embryos. After one minute, embryos were transferred to a new plate of Ringer's solution. Embryos were rotated ventral side up, held in place with an insect poker by the head, and sliced from neck to abdomen using another insect poker to loosen the myofibers. Embryo is then turned over and shaken to pour out the fibers. Isolated fibers can be transferred using a P20 pipette.

Crude Myosin extraction and SDS-PAGE gel

For crude Myosin extraction, 20 embryos sorted *mylpfa*$^{-/-}$ mutant or wild-type by their swimming defects and birefringence were deyolked and lysed in liquid nitrogen. Myosins were enriched by following a modified protocol for extracting myosins from a chicken muscle (Racusen and Thompson, 1997). Myosins were extracted in a high salt buffer and further enriched by dilution in water to allow for polymerization of the heavy chains, leading to insolubility. To minimize protein degradation, all extractions were performed on ice. Myosin pellets were suspended in 50 microliters and 10 microliters were run on a Bolt 4-12% Bis-Tris Plus Acrylamide gel (BG04125) at 100 v until dye reaches the bottom.

Acknowledgements

Many individuals were instrumental to putting together all of this data and helping me throughout my undergraduate project. Other than myself, Jared Talbot, Pooja Gangras, and Sarah Shepherd were integral in the construction of the Myosin light chain mutant zebrafish lines. I'd also like to thank Kimberly Hromowyk, Brit Martin, Amy Li, and David Warshaw for their expertise, time, and assistance in characterizing aspects of the *mylpfa*$^{-/-}$ mutant phenotype.

I'd like to thank the many individuals that helped me through my undergraduate research career. I'd like to thank Sharon Amacher for accepting me into her lab back in my freshman year before I had even taken a genetics course. She has been a caring and knowledgeable mentor throughout my time in the lab and I will always look back on my time fondly. I am so grateful for my great mentor, Jared Talbot, who has taught me everything from how to pipette to how to design and think about the next steps to a project. He also provided his artistic skills in illustrating the cartoons shown in figures 1, 2 and 7. The other members of the Amacher lab have always been quick to help if I needed it, supportive in lab meetings, and welcoming to me. I feel very fortunate to have found such a genuinely kind, supportive, and intelligent lab to work in. My work at Sharon Amacher's lab has helped me to become a better student, a better scientist, and has been instrumental to my undergraduate career. I am so glad to be able to share all the work I've done the past three and a half years in the lab.

References

Burghardt, T.P., Ajtai, K., Sun, X., Takubo, N., and Wang, Y. (2016). In vivo myosin step-size from zebrafish skeletal muscle. Open Biol. *6*.

Clark, K.A., McElhinny, A.S., Beckerle, M.C., and Gregorio, C.C. (2002). Striated muscle cytoarchitecture: an intricate web of form and function. Annu. Rev. Cell Dev. Biol. *18*, 637–706.

Du, A., Sanger, J.M., Linask, K.K., and Sanger, J.W. (2003). Myofibrillogenesis in the first cardiomyocytes formed from isolated quail precardiac mesoderm. Dev. Biol. *257*, 382–394.

Duggal, D., Nagwekar, J., Rich, R., Huang, W., Midde, K., Fudala, R., Das, H., Gryczynski, I., Szczesna-Cordary, D., and Borejdo, J. (2015). Effect of a myosin regulatory light chain mutation K104E on actin-myosin interactions. Am. J. Physiol. - Heart Circ. Physiol. *308*, H1248–H1257.

Elworthy, S., Hargrave, M., Knight, R., Mebus, K., and Ingham, P.W. (2008). Expression of multiple slow myosin heavy chain genes reveals a diversity of zebrafish slow twitch muscle fibres with differing requirements for Hedgehog and Prdm1 activity. Development *135*, 2115–2126.

Haines, L., Neyt, C., Gautier, P., Keenan, D.G., Bryson-Richardson, R.J., Hollway, G.E., Cole, N.J., and Currie, P.D. (2004). Met and Hgf signaling controls hypaxial muscle and lateral line development in the zebrafish. Dev. Camb. Engl. *131*, 4857–4869.

von Hofsten, J., Elworthy, S., Gilchrist, M.J., Smith, J.C., Wardle, F.C., and Ingham, P.W. (2008). Prdm1- and Sox6-mediated transcriptional repression specifies muscle fibre type in the zebrafish embryo. EMBO Rep. *9*, 683–689.

Hogarth, M.W., Houweling, P.J., Thomas, K.C., Gordish-Dressman, H., Bello, L., Pegoraro, E., Hoffman, E.P., Head, S.I., and North, K.N. (2017). Evidence for ACTN3 as a genetic modifier of Duchenne muscular dystrophy. Nat. Commun. *8*, 14143.

Huxley, A.F. (2000). Cross-bridge action: present views, prospects, and unknowns. J. Biomech. *33*, 1189–1195.

Hwang, P.M., and Sykes, B.D. (2015). Targeting the sarcomere to correct muscle function. Nat. Rev. Drug Discov. *14*, 313–328.

Ignatius, M.S., Chen, E., Elpek, N.M., Fuller, A.Z., Tenente, I.M., Clagg, R., Liu, S., Blackburn, J.S., Linardic, C.M., Rosenberg, A.E., et al. (2012). In vivo imaging of tumor-propagating cells, regional tumor heterogeneity, and dynamic cell movements in embryonal rhabdomyosarcoma. Cancer Cell *21*, 680–693.

Jiang, P., Song, J., Gu, G., Slonimsky, E., Li, E., and Rosenthal, N. (2002). Targeted Deletion of the MLC1f/3f Downstream Enhancer Results in Precocious MLC Expression and Mesoderm Ablation. Dev. Biol. *243*, 281–293.

Jowett, T. (1999). Analysis of protein and gene expression. Methods Cell Biol. *59*, 63–85.

Kimmel, C.B., Ballard, W.W., Kimmel, S.R., Ullmann, B., and Schilling, T.F. (1995). Stages of embryonic development of the zebrafish. Dev. Dyn. Off. Publ. Am. Assoc. Anat. *203*, 253–310.

Lemke, S.B., and Schnorrer, F. (2017). Mechanical forces during muscle development. Mech. Dev. *144*, 92–101.

Lin, B.L., Li, A., Mun, J.Y., Previs, M.J., Previs, S.B., Campbell, S.G., dos Remedios, C.G., Tombe, P. de P., Craig, R., Warshaw, D.M., et al. (2018). Skeletal myosin binding protein-C isoforms regulate thin filament activity in a Ca2+-dependent manner. Sci. Rep. *8*.

Lowey, S., Waller, G.S., and Trybus, K.M. (1993a). Skeletal muscle myosin light chains are essential for physiological speeds of shortening. Nature *365*, 454.

Lowey, S., Waller, G.S., and Trybus, K.M. (1993b). Function of skeletal muscle myosin heavy and light chain isoforms by an in vitro motility assay. J. Biol. Chem. *268*, 20414–20418.

Martin, B.L., Gallagher, T.L., Rastogi, N., Davis, J.P., Beattie, C.E., Amacher, S.L., and Janssen, P.M.L. (2015). In vivo assessment of contractile strength distinguishes differential gene function in skeletal muscle of zebrafish larvae. J. Appl. Physiol. Bethesda Md 1985 *119*, 799–806.

Meredith, C., Herrmann, R., Parry, C., Liyanage, K., Dye, D.E., Durling, H.J., Duff, R.M., Beckman, K., de Visser, M., van der Graaff, M.M., et al. (2004). Mutations in the slow skeletal muscle fiber myosin heavy chain gene (MYH7) cause laing early-onset distal myopathy (MPD1). Am. J. Hum. Genet. *75*, 703–708.

Morrow, Z.T., Maxwell, A.M., Hoshijima, K., Talbot, J.C., Grunwald, D.J., and Amacher, S.L. (2017). tbx6l and tbx16 are redundantly required for posterior paraxial mesoderm formation during zebrafish embryogenesis: Zebrafish T-Box Genes and Somitogenesis. Dev. Dyn. *246*, 759–769.

Racusen, R. H. and K. V. Thompson. 1996. Isolation of myosin and actin from chicken muscle. Pages 97-111,in Tested studies for laboratory teaching, Volume 18 (J. C. Glase, Editor). Proceedings of the 18th Workshop/Conference of the Association for Biology Laboratory Education (ABLE), 322 pages.

Rauch, G.J., Lyons, D.A., Middendorf, I., Friedlander, B., Arana, N., Reyes, T., and Talbot, W.S. (2003) Submission and Curation of Gene Expression Data. ZFIN Direct Data Submission. . (http://zfin.org).

Sanger, J.W., Wang, J., Fan, Y., White, J., and Sanger, J.M. (2010). Assembly and Dynamics of Myofibrils.

Sanger, J.W., Wang, J., Fan, Y., White, J., Mi-Mi, L., Dube, D.K., Sanger, J.M., and Pruyne, D. (2017). Assembly and Maintenance of Myofibrils in Striated Muscle. Handb. Exp. Pharmacol. *235*, 39–75.

Scheid, L.-M., Weber, C., Bopp, N., Mosqueira, M., and Fink, R.H.A. (2017). Extraction Protocols for Individual Zebrafish's Ventricle Myosin and Skeletal Muscle Actin for In vitro Motility Assays. Front. Physiol. *8*.

Schiaffino, S., and Reggiani, C. (2011). Fiber types in mammalian skeletal muscles. Physiol. Rev. *91*, 1447–1531.

Schilling, T.F., and Kimmel, C.B. (1997). Musculoskeletal patterning in the pharyngeal segments of the zebrafish embryo. Dev. Camb. Engl. *124*, 2945–2960.

Sharma, M.C., and Goebel, H.H. (2005). Protein aggregate myopathies. Neurol. India *53*, 273–279.

Takashima, S. (2009). Phosphorylation of myosin regulatory light chain by myosin light chain kinase, and muscle contraction. Circ. J. Off. J. Jpn. Circ. Soc. *73*, 208–213.

Talbot, J.C., and Amacher, S.L. (2014). A streamlined CRISPR pipeline to reliably generate zebrafish frameshifting alleles. Zebrafish *11*, 583–585.

Talbot, J.C., Johnson, S.L., and Kimmel, C.B. (2010) hand2 and Dlx genes specify dorsal, intermediate and ventral domains within zebrafish pharyngeal arches. Development (Cambridge, England). 137(15):2507-2517.

Talbot, J.C., and Maves, L. (2016). Skeletal muscle fiber type: using insights from muscle developmental biology to dissect targets for susceptibility and resistance to muscle disease. Wiley Interdiscip. Rev. Dev. Biol. *5*, 518–534.

Tang, Q., Moore, J.C., Ignatius, M.S., Tenente, I.M., Hayes, M.N., Garcia, E.G., Torres Yordán, N., Bourque, C., He, S., Blackburn, J.S., et al. (2016). Imaging tumour cell heterogeneity following cell transplantation into optically clear immune-deficient zebrafish. Nat. Commun. *7*, 10358.

Thisse, B., Pflumio, S., Fürthauer, M., Loppin, B., Heyer, V., Degrave, A., Woehl, R., Lux, A., Steffan, T., Charbonnier, X.Q. and Thisse, C. (2001) Expression of the zebrafish genome during embryogenesis (NIH R01 RR15402). ZFIN Direct Data Submission (http://zfin.org).

Thisse, B., Thisse, C. (2004) Fast Release Clones: A High Throughput Expression Analysis. ZFIN Direct Data Submission. . (http://zfin.org).

Wang, Y., Szczesna-Cordary, D., Craig, R., Diaz-Perez, Z., Guzman, G., Miller, T., and Potter, J.D. (2007). Fast skeletal muscle regulatory light chain is required for fast and slow skeletal muscle development. FASEB J. *21*, 2205–2214.

Wang, Y., Ajtai, K., Kazmierczak, K., Szczesna-Cordary, D., and Burghardt, T.P. (2016). N-Terminus of Cardiac Myosin Essential Light Chain Modulates Myosin Step-Size. Biochemistry (Mosc.) *55*, 186–198.

Weitkunat, M., Brasse, M., Bausch, A.R., and Schnorrer, F. (2017). Mechanical tension and spontaneous muscle twitching precede the formation of cross-striated musclein vivo. Dev. Camb. Engl. *144*, 1261–1272.

Xu, Y., He, J., Wang, X., Lim, T.M., and Gong, Z. (2000). Asynchronous activation of 10 muscle-specific protein (MSP) genes during zebrafish somitogenesis. Dev. Dyn. Off. Publ. Am. Assoc. Anat. *219*, 201–215.